Compressive strength of composite laminates with terminated internal plies

Craig A. Steeves, Norman A. Fleck*

Engineering Department, Cambridge University, Trumpington Street, Cambridge CB2 1PZ, UK

Abstract

Composite laminates are commonly tapered by terminating internal prepreg plies, creating geometrical defects which can induce failure. In this study, experiments have been conducted on tapered laminates loaded in axial compression. Failures by microbuckling or delamination were observed to nucleate near the dropped plies. The results indicate that existing models of microbuckling give adequate predictions of strength in specimens with mild geometric defects, while a new model given here for delamination provides satisfactory predictions of strength for more severe defects.
© 2004 Elsevier Ltd. All rights reserved.

Keywords: A. Laminates; B. Delamination; B. Microstructure; C. Micro-mechanics

1. Introduction

Components made of composite laminates often vary in thickness from one part of the component to another. Because composite laminates are frequently made from prepregs of discrete thickness, it is not possible to taper a laminate continuously. Instead, the usual way that tapering is achieved is by terminating one or more of the internal plies during prepreg lay-up. This technique produces a geometry as sketched and shown in the photograph of Fig. 1. The terminated internal plies give rise to a large triangular resin pocket, with the plies above this resin pocket misaligned relative to the axial direction of the laminate. The effect of these geometrical imperfections on the compressive strength of the laminate will be studied here.

Several authors have addressed the problem of a composite containing dropped plies and loaded in tension by analysing the entire cross-sectional element containing the terminated plies. Fish and Lee [7] concluded that the strength of the specimen was best predicted by a maximum shear stress failure criterion. Salpekar et al. [15] suggested

that fracture-mechanics criteria were more accurate. Wisnom et al. [4–6,16,17] studied composites with terminated internal plies loaded in tension. Their results suggested that two failure regimes were operative. For composites without terminated internal plies or other microstructural details which would generate large internal stress concentrations, stress-based failure criteria were preferable, while for composites with large stress concentrations, fracture-mechanics-based failure criteria gave better predictions. Mukherjee and Varughese [14] and Her [10] have developed specialised finite elements which allow the modelling of ply drops. Kairouz and Heath [13] have tested specimens in tension and compared the experimental results to finite element models. They reported that cracks appeared from the resin-rich pocket and propagated stably under increasing applied stress. Kairouz and Ball [12] used numerical models to predict the stress concentration factors in composites with terminated plies loaded in compression, and used the stress concentration factors in conjunction with the tensile strength of a unidirectional laminate to predict failure stresses. Experiments showed that these predictions were slightly non-conservative (high by 9%).

Compression-driven delamination of the surface laminae is a possible cause of failure for ply-drop specimens in compression. Chai et al. [3] presented a one-dimensional

---

* Corresponding author. Tel.: +44 1223 332 650; fax: +44 1223 332 662.

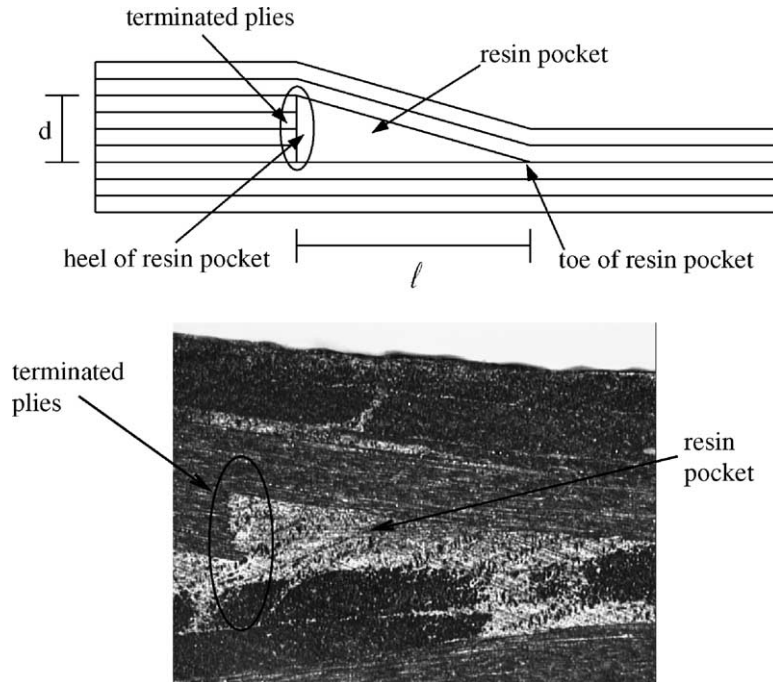*E-mail address:* naf1@eng.cam.ac.uk (N.A. Fleck).

Fig. 1. Sketch and micrograph of terminated internal plies. Each ply is 0.125 mm thick.

model of the delamination of a thin film from a semi-infinite substrate due to the presence of a pre-existing interfacial crack. This model was developed further by Hutchinson and Suo [11]. These analyses indicate that for bifurcation buckling of the surface layer from an initially closed crack, the strain energy release rate is zero until the surface layer has buckled away from the substrate. In the case of terminated internal plies as studied here, the surface plies are already deformed, and this geometric imperfection causes the strain energy release rate to be positive at any finite value of compressive stress.

2. Experimental procedure

In this experimental investigation, the compressive strength of composite laminates with dropped plies was determined as a function of local geometry near the terminated plies. Results for macroscopic bending, with the terminated plies on the compressive face, are compared with results for uniaxial compression.
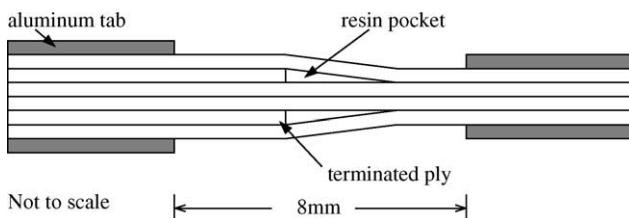

Fig. 2. Sketch of symmetrical ply-drop specimens.

2.1. Uniaxial compression tests

2.1.1. Specimens

All specimens for the direct compression tests comprised unidirectional $0°$ laminates made from 0.125 mm thick T300/914C carbon fibre–epoxy prepregs. The specimens were laid up by hand and autoclaved using the recommended schedule.[1] The consistency of the ply-drop geometry was assured by using additional plies of prepreg as temporary tooling, as suggested by Wisnom et al. [17]. A sketch of the overall geometry is shown in Fig. 2, with two ply-drop regions arranged symmetrically about the mid-plane. Four specimen geometries were manufactured and tested in order to vary the physical size and the taper angle α of the ply drop, as shown in Fig. 3. The tooling ensures that the inclined plies are 1 mm long for each group of terminated plies. The four specimen geometries are:

(A) no terminated plies—'control'
(B) two terminated plies per side—'shallow taper'
(C) four terminated plies per side—'steep taper'
(D) four terminated plies per side, arranged in a step pattern—'staggered taper'

The total fibre misalignment in any specimen is taken to be the sum of the inherent fibre waviness, $\bar{\phi}$, as measured by
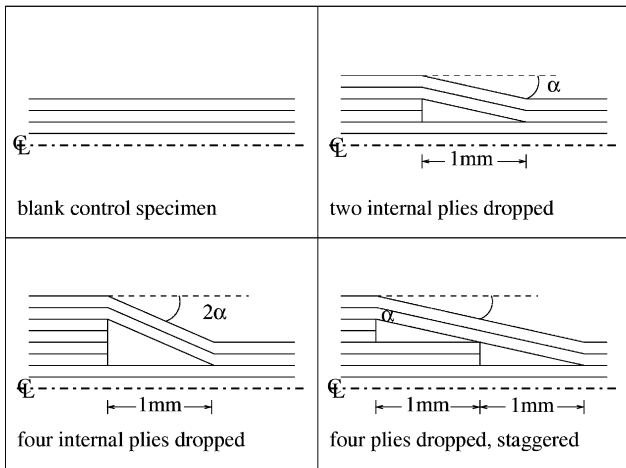

Fig. 3. Sketch of specimen geometry for direct compression tests (not to scale). All specimens are symmetric about the mid-plane. Individual plies are 0.125 mm thick.

Yurgartis [18] to be at most 3°, plus the angle of the taper, α. Table 1 gives the geometrical specifications for the four specimen types.

After autoclaving, the plates were cut into coupons and ground to a nominal width of 10 mm. Aluminium tabs of length 65 mm and thickness 1 mm were bonded to the ends of the specimen, as shown in Fig. 2, using Hexcel Redux 322 epoxy adhesive leaving a gauge length of 8 mm. For the case of the control specimens, 1 mm long strain gauges were bonded to each side of the test specimen in the gauge length and protected by liquid latex. The test results were disregarded when the strain gauge readings on the two sides of the specimen diverged significantly, indicating large bending strains. It was not possible to apply strain gauges to the tapered specimens due to their short gauge length, and to the difficulty of applying strain gauges on top of the ply drops.

2.1.2. Test procedure

Direct compression tests were carried out using the Celanese compression rig. This apparatus consists of a series of nested cylinders and cones, as sketched in Fig. 4. The test specimen is gripped in the jaws of the Celanese rig, and the compressive force is transmitted to the test specimen by shear stresses only, eliminating the problem of brooming of the end of a compressive specimen.
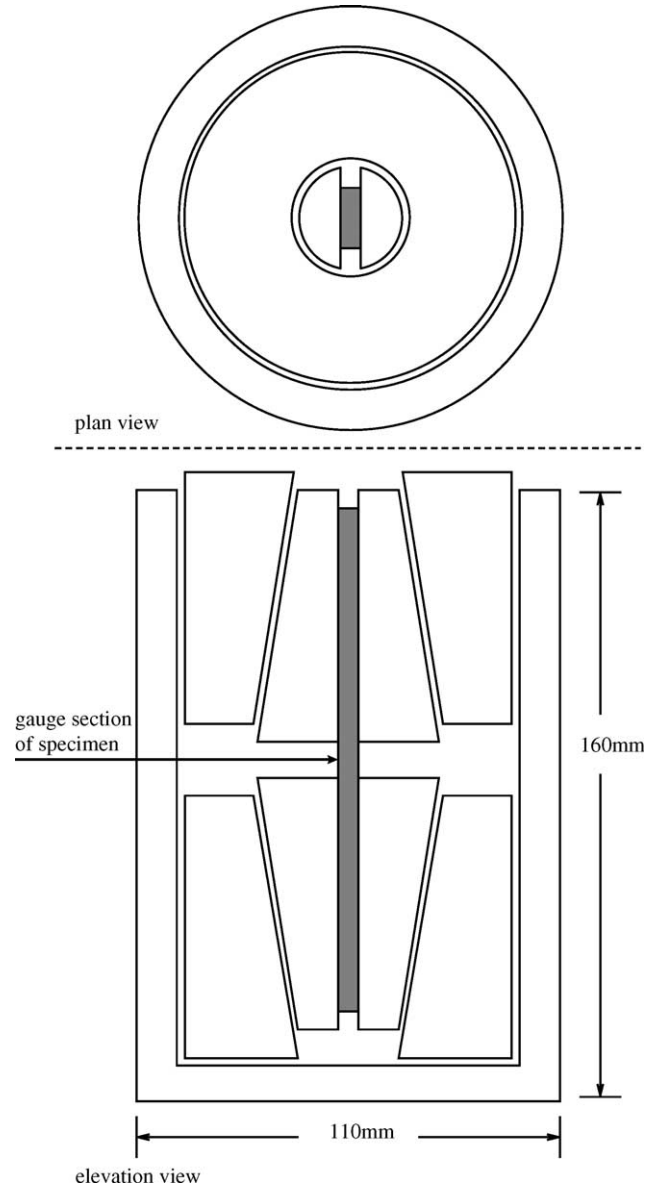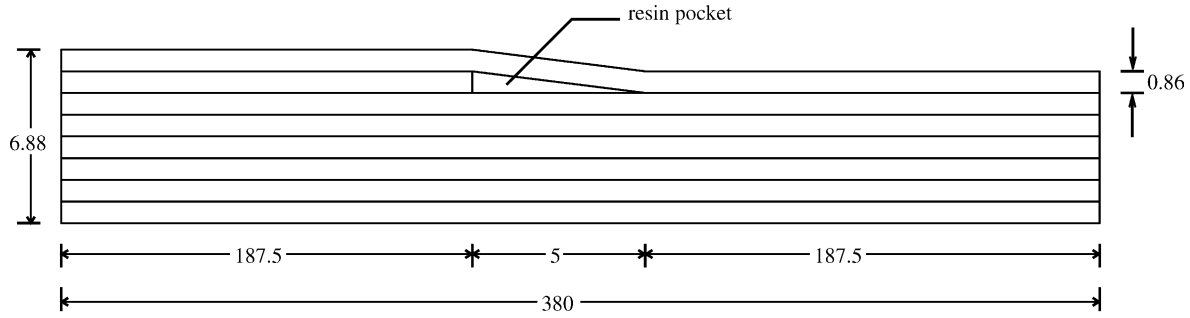

Fig. 4. Sketch of Celanese rig.

The rig, with specimen, was loaded in compression in a screw-driven Instron 5501R test frame. The strain gauges adhered to the control specimens were monitored to ensure that bending of the specimen was minimised. All specimens were loaded to failure at a cross-head speed of 0.5 mm/min.

2.2. Bend tests

2.2.1. Specimens

Plates of tapered composite laminate were provided by British Aerospace–Airbus. The plates were manufactured from T300/914C carbon fibre–epoxy prepregs, which had been stitched together in four-ply blankets for ease of manufacture. Each blanket comprised the configuration

Table 1
Geometry of ply drop specimens

Specimen type	Plies in thick section	Nominal thickness (mm)	Plies in thin section	Nominal thickness (mm)	Taper angle (degrees)
Control	8	1.0	8	1.0	0
Shallow taper	12	1.5	8	1.0	7
Steep taper	16	2.0	8	1.0	14
Staggered	16	2.0	8	1.0	7

Fig. 5. Sketch of laminate lay-up used in four-point bending tests.

[$0_2°, \pm45°$] and was 0.86 mm thick. This configuration was chosen as it was practically representative of non-crimp fabrics, and hence the ply thickness is not the same as for the uniaxial test specimens. The overall geometry of these plates is shown in Fig. 5. The thick section of each plate consisted of eight blankets of the prepreg fabric, arranged in the configuration $[[[\pm45°,0_2°]_s]_s]_s$. To produce the thin section, the second blanket was terminated at the point shown in Fig. 5.

To produce specimens, 10 mm wide beams were cut from the plates using a diamond grit saw. Strain gauges were bonded to the specimen using cyanoacrylate adhesive at the location shown in Fig. 6 and as enumerated in Table 2.

2.2.2. Test procedure

The specimens were tested in a four-point bend rig using the screw-driven Instron test frame so that the face of the specimen with the dropped plies was in compression. The bend rig was set up so that the distance between the outer support rollers was 350 mm, while the spacing of the inner loading rollers was 120 mm. All rollers were of diameter 20 mm. The specimens were loaded with a cross-head displacement rate of 2 mm/min, and the load, cross-head displacement and strains were logged by a computer.

Fig. 6. Sketch of locations for strain gauges.

Four specimens, numbered 1–4, were loaded to failure. Specimen 5 was loaded to 90% of predicted failure load and the test was then arrested. Specimen 6 was loaded until an acoustic emission was heard, and then the test was halted.

2.3. In situ tests in the scanning electron microscope (SEM)

The purpose of the tests within the scanning electron microscope was not to collect quantitative data about the behaviour of tapered laminates in compression, but rather to locate the initiation site for failure.

2.3.1. Specimens

Composite plates similar to those used in the direct compression testing were prepared for in situ compressive loading within the scanning electron microscope. These plates were also symmetrical about their mid-plane, but contained only six prepreg plies in the thick section, and four plies in the thin section, with one ply dropped on each side of the specimen. This produced an angle of taper, α of 7°, equal to the shallow taper specimens and staggered taper specimens. Coupons approximately 10 mm long and 6 mm wide were cut from the composite plate. The ends of the coupons were fixed in machined brass fittings using quick-setting epoxy adhesive.

2.3.2. Test procedure

The coupons in their brass fittings were loaded to failure in a test rig designed for use in the scanning electron microscope. This test rig allows real-time electron microscope images to be taken during loading of the test
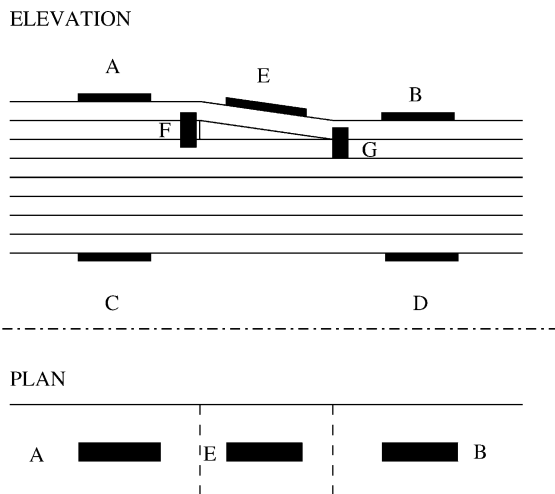
Table 2
Strain gauge placement on bend specimens

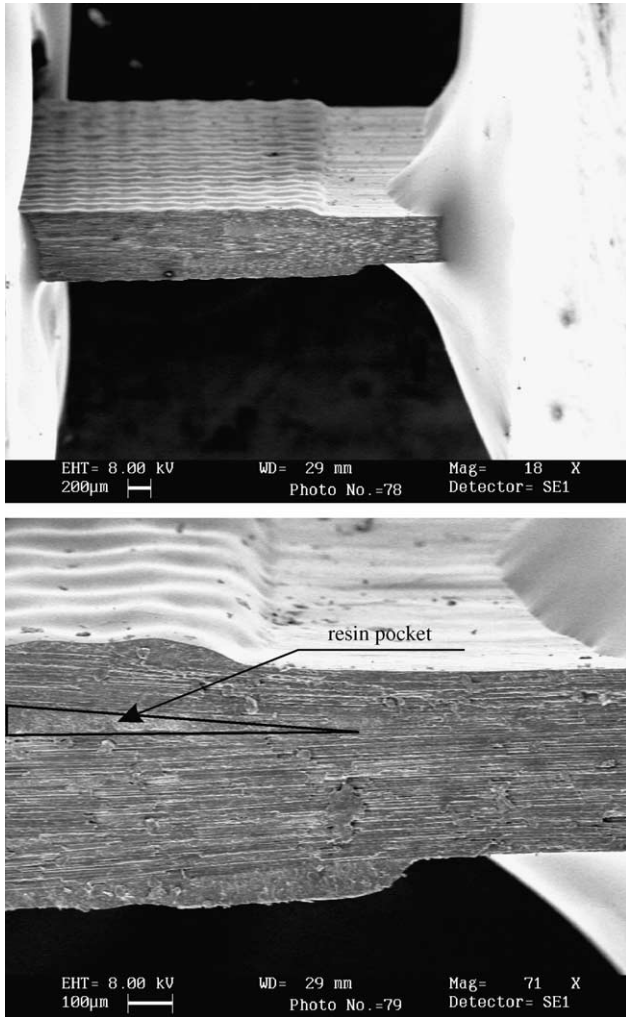| Specimen	Locations
1	A,B,C,D,E
2	A,B,C,D,F,G
3	A,B,C,D,F,G
4	A,B,C,D
5	A,B,C,D,E
6	A,B,C,D,F,G

Fig. 7. Specimen for SEM testing, large view (top) and close-up view (bottom) with the location of the resin pocket shown.

specimen. The compressive loading rate was varied during the tests to allow both video tape recording and still image capture at various times. The test rig is sufficiently stiff for the degree of additional damage post peak load to be limited; consequently, the failed specimens could be examined for evidence of the operative mode of failure.

Fig. 7 shows a specimen mounted in the SEM but prior to testing. The upper image is a large view of the specimen showing the brass grips, while the lower image is a close-up of the ply-drop region, where one of the resin pockets is clearly visible.

3. Experimental results

3.1. Compression tests

Table 3 gives the results of the direct compression tests on the tapered and control specimens. Stresses are calculated in the thin section of the laminate. In the cases

Table 3
Experimental results for direct compressions tests

Specimen	Specimen number	Failure stress (MPa)	Average strength (MPa)	Standard deviation (MPa)
Control	1	1473		
	2	1538		
	3	1314		
	4	1599		
	5	1745	1511	157
	6	1439		
	7	1670		
	8	1311		
Shallow taper	1	1003		
	2	1046		
	3	1037	1017	23.4
	4	983		
Steep taper	1	643		
	2	712		
	3	851	745	89
	4	775		
Staggered taper	1	1053		
	2	1111		
	3	923	1020	81
	4	993		

of the control specimens and the shallow and staggered taper specimens, as defined in Table 1, failure occurred by fibre microbuckling and was sudden and catastrophic. In these cases, severe damage accompanied the failure. For the specimens with a steep taper, there was less damage after failure. In three steeply tapered specimens, failure was accompanied by both delamination and fibre fracture; exceptionally, for the steeply tapered specimen number 2, the only observable damage was delamination near the resin pocket.

The measured compressive strength of the four geometries is plotted in Fig. 8 as a function of the total initial fibre misalignment, $\bar{\phi} + \alpha$. It is assumed that the maximum
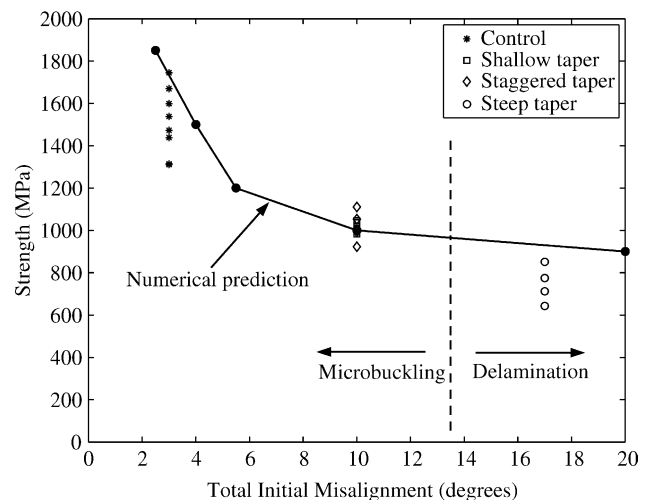

Fig. 8. Relationship between strength and initial fibre misalignment angle.

misalignment angle for unidirectional composites is approximately 3°, following Yurgartis [18]. This gives a total initial misalignments of 3° for the control specimens, 10° for the shallow taper and staggered specimens, and 17° for the steeply tapered specimens.

3.2. Bend tests

Failure in four-point bending occurred suddenly and catastrophically, with a drop in load of approximately 50% and multiple delaminations surrounding the resin-rich pocket. In one instance, specimen 3, post-test examination of the videotaped test revealed that a surface ply had delaminated approximately 3 s prior to final failure. This coincided with a small drop in the load.

Using the strain gauge data from the top and bottom of the thin section (positions B and D in Fig. 6) and assuming that the axial strain is distributed linearly across the section of the specimen, it is possible to infer strains at any point of the cross-section. Given the elastic modulus of the plies at any position, the local stress can also be inferred. Thus, the local stress, σ, can be calculated by

$$\sigma = E\left(\epsilon_t + (\epsilon_b - \epsilon_t)\left(\frac{d_t}{t_l}\right)\right) \qquad (1)$$

where E is the elastic modulus of the plies at depth d_t from the top of the laminate, t_l is the total laminate thickness at this position, and ε_t and ε_b are the measured axial strains at the top and bottom surfaces of the laminate, respectively.

Plots of bending moment per unit width versus the inferred stress in the uppermost unidirectional ply of the thin section of the beam are shown in Fig. 9 for specimens 1–4. The stress is calculated using Eq. (1) at a depth below the top of the laminate of 0.66 mm, which is the middle of the 0° plies in the uppermost blanket of the laminate. It is this blanket which is misaligned over the resin pocket due to the terminated plies. This blanket was chosen according to
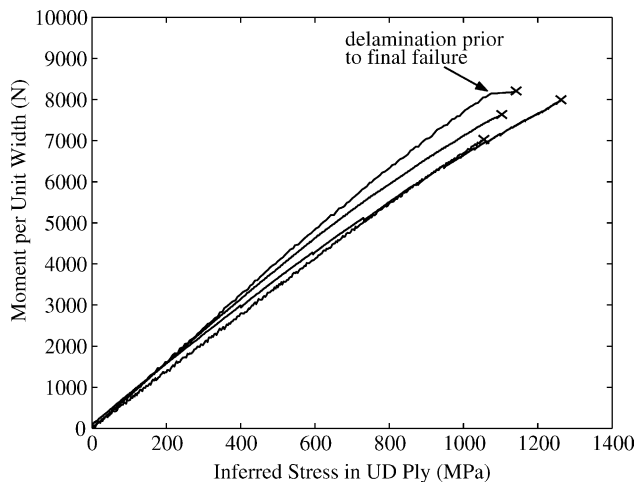

Fig. 9. Plot of inferred stress vs. load per unit width for four ply drop bending specimens tested to failure.
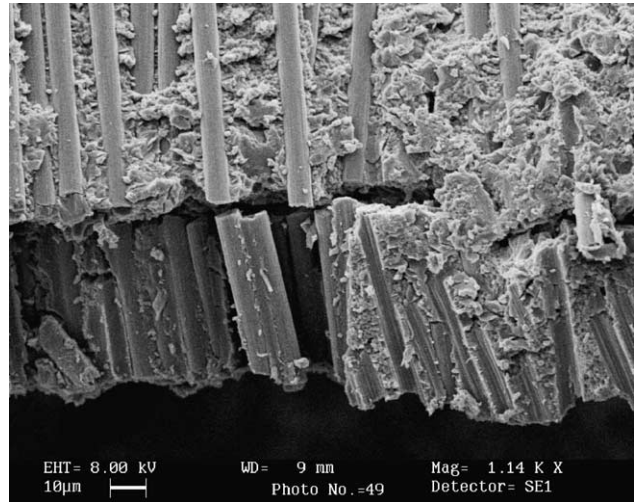

Fig. 10. SEM image of microbuckle band found near toe of resin pocket in specimen 1.

the hypothesis that failure in these laminates occurs by microbuckling of the most highly misaligned 0° fibres. These data give inferred stresses at failure of approximately 1100–1200 MPa. This level of stress is close to the measured failure strength of the shallow taper uniaxial specimens comprising 0° fibres; recall Table 3.

Specimen 1 was sectioned after testing, and the pieces were gold-coated and examined in a scanning electron microscope. Fig. 10 shows an SEM image of a microbuckle band which was found near the toe of the resin pocket. A large amount of delamination and microbuckling accompanied failure in the bend tests, and this made it impossible to confirm that this microbuckle initiated failure.

Both tests 5 and 6 were halted before final failure, and the specimens were sectioned to search for damage; in neither case was damage evident.

3.3. In situ tests in the scanning electron microscope

Fig. 11 shows electron micrographs of a tapered specimen after failure. This specimen has the same angle of taper as that of the shallow taper specimens and the staggered taper specimens. The top image shows the microbuckle band immediately after failure. It is clear that the microbuckle band has formed at the toe of the upper resin pocket. The lower image is the same specimen after one half of the failed specimen was removed and the remainder was gold-coated for better imaging. The resin pocket is clearly visible. The only observable damage is the microbuckle band evident at the resin pocket. This is contrary to the suggestion of Cui et al. [6] that compressive failure requires delamination.

4. Discussion

The results of this study suggest that the compressive strength of tapered composite laminates is dictated by two
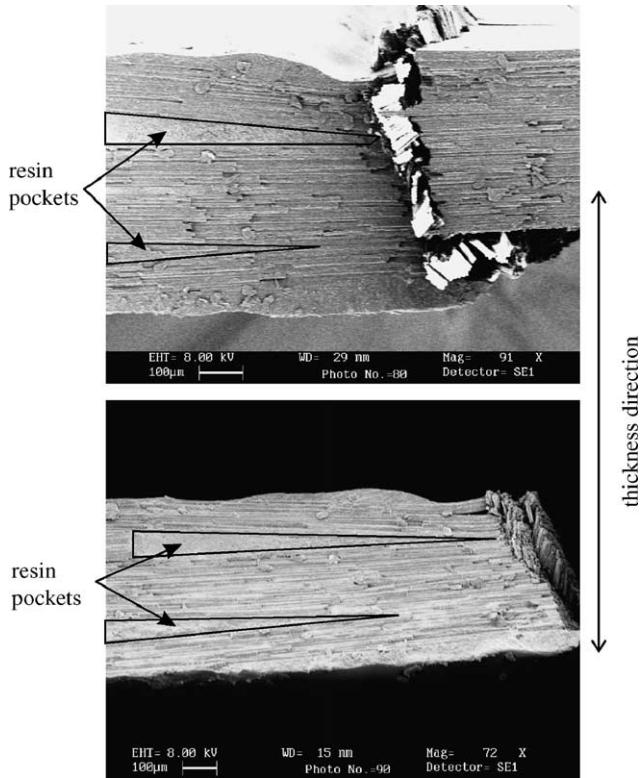
Fig. 11. Electron micrographs of specimen from dynamic SEM test: after failure in situ (top) and after removal and recoating (bottom).

competing modes of failure. The first mode of failure is fibre microbuckling, and is governed by the induced fibre waviness of longitudinal fibres in the vicinity of the ply drop. The second mode of failure is delamination cracking. Each phenomenon is discussed in turn.

4.1. Fibre microbuckling

For all specimens with terminated internal plies, the dominant geometric parameters are the height of the dropped plies, d, and the length of the region over which they are dropped, ℓ, as shown in Fig. 1. It is generally accepted that microbuckling of fibre composites is highly sensitive to the initial misalignment of the longitudinal fibres. In the case of dropped plies, the initial misalignment angle is given by $\bar{\phi} + \alpha$, where α is adequately approximated by:

$$\alpha = \frac{d}{\ell} \qquad (2)$$

The theoretical study of Liu and Fleck [8] indicates that, for regions of fibre waviness of size similar to those observed here, the relationship between compressive strength and fibre waviness is that shown in Fig. 8. Their numerical study, based upon the work of Budiansky and Fleck [2] and Fleck and Shu [9], was for unidirectional composites with circular patches of fibre waviness of radius equal to 200 fibre diameters. Good agreement exists

between the predicted and measured strengths for the specimens of total misalignment angle 3 and 10°. The in situ scanning electron microscope tests on specimens of shallow taper confirm that microbuckles form in the region of the toe of the resin pocket, see Fig. 11. Delamination was absent in these specimens. It is concluded that the active failure mode in the ply-drop specimens of shallow taper is microbuckling of the longitudinal fibres near the toe of the resin pocket. In contrast, the specimens with a steep taper (17° total misalignment) failed by ply delamination, and the measured compressive strength falls below the microbuckling prediction.

4.2. Ply delamination

The symmetrical specimens with 17° total initial misalignment angle failed by delamination rather than by microbuckling according to the following argument. Fig. 8 shows that these specimens failed at a lower stress than predicted by microbuckling theory. In addition, delamination was found in all of these specimens, while microbuckling was not. It is concluded that ply delamination was the dominant mode of failure. The Chai model is not directly applicable to the delamination problem studied here as the Chai model predicts that a positive strain energy release rate only exists after the surface film has buckled. For the case of dropped plies, the geometric imperfection in the form of an initial curvature of the surface film implies that a positive strain energy release rate exists immediately upon loading. Consequently, an alternate analysis is necessary for the case of compression-driven delamination.

A simple model of compressive stress-driven delamination is presented here. Fig. 12 shows the local region around terminated internal plies. The height of the dropped plies, as noted previously, is d, while the length of the resin pocket is ℓ. This simple model considers only the top plies of the specimen, and models them as a membrane with an applied axial stress. A membrane which is subjected to an axial stress σ_a and has curvature κ will also have induced transverse stress σ_t to maintain equilibrium, as shown in Fig. 12. The relationship between the axial stress and the transverse stress is
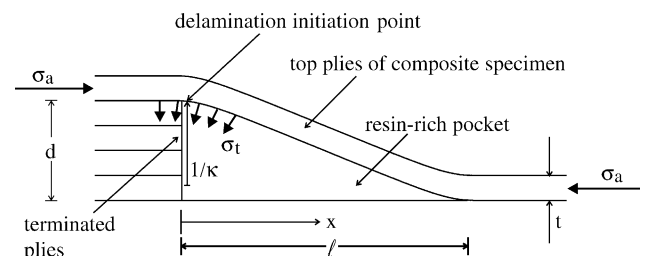
$$\sigma_t = \sigma_a t \kappa \qquad (3)$$

Fig. 12. Geometry involved in compressive stress-driven delamination.

Table 4
Predicted compressive strengths of tapered laminates for failure by delamination and by microbuckling

Specimen	Measured curvature (mm^{-1})	Delamination strength (MPa)	Fibre angle (degrees)	Microbuckle strength (MPa)	Measured strength (MPa)
Shallow	0.29	1041	10	1000	1017
Steep	0.58	694	17	920	745
Staggered	0.22	1810	10	1000	1020

Strength is given as the stress in the thin section of the laminate.

where t is the thickness of the membrane and κ is the local curvature of the membrane.

For the geometry of the ply drop, the critical region is at the heel of the resin pocket, where the transverse stresses will be tensile. The axial stress σ_a can be estimated as the axial stress in the thick section of the ply-drop specimen for which the transverse stress σ_t attains the through-thickness tensile strength. The curvature of the outermost plies can be measured from micrographs. The through-thickness tensile strength of the laminates has been measured independently to be 50 MPa [1]. Assembling these data gives the predictions and measured strengths listed in Table 4, with the compressive strength defined as the axial stress in the thin section of the laminate at failure. The predicted strength for microbuckling failure is included in the table. In each case, the expected failure mechanism is that which gives the lower predicted strength.

It is clear from both Table 4 and Fig. 8 that microbuckling is both predicted and observed for the shallow taper and staggered taper specimens. In contrast, delamination is the predicted and observed mode of failure for the steeply tapered specimens. Furthermore, the quantitative predictions of failure stress are within 10% for all specimens tested here.

5. Concluding remarks

Composite laminates with terminated internal plies fail either by microbuckling of the longitudinal fibres near the toe of the resin pocket, or by delamination near the heel of the resin pocket. Microbuckling is active for shallow angles of taper while delamination dominates in steeply tapered specimens. Existing models of microbuckling give accurate predictions of compressive strength and bend strength for laminates where microbuckling failure is critical. Both the delamination model and the microbuckling model give adequate predictions of compressive strength in their respective regimes of dominance.

References

[1] Anon. NCF stage 2 option 0 T300/914C material properties. Technical report. British Aerospace, Airbus Division; 1997.
[2] Budiansky B, Fleck NA. Compressive failure of fibre composites. J Mech Phys Solids 1993;41(1):183–211.
[3] Chai H, Babcock CD, Knauss WG. One dimensional modelling of failure in laminated plates by delamination buckling. Int J Solids Struct 1981;17(11):1069–83.
[4] Cui W, Wisnom MR. A combined stress-based and fracture-mechanics-based model for predicting delamination in composites. Composites 1993;24(6):467–74.
[5] Cui W, Wisnom MR, Jones M. A comparison of failure criteria to predict delamination of unidirectional glass/epoxy specimens waisted through the thickness. Composites 1992;23(3):158–66.
[6] Cui W, Wisnom MR, Jones M. New model to predict static strength of tapered laminates. Composites 1995;26(2):141–6.
[7] Fish JC, Lee SW. Delamination of tapered composite structures. Eng Fract Mech 1989;34:43–54.
[8] Fleck NA, Liu D. Microbuckle initiation from a patch of large amplitude fibre waviness in a composite under compression and bending. Eur J Mech A/Solids 2001;20:23–37.
[9] Fleck NA, Shu JY. Microbuckle initiation in fibre composites: a finite element study. J Mech Phys Solids 1995;43(12):1887–918.
[10] Her S-C. Stress analysis of ply drop-off in composite structures. Compos Struct 2002;57(1–4):235–44.
[11] Hutchinson JW, Suo Z. Mixed mode cracking in layered materials. Adv Appl Mech 1992;29:63–191.
[12] Kairouz KC, Ball J. Three-dimensional finite element analysis of ply drop-offs in composite structures. Technical report. British Aerospace Air-bus; 1997.
[13] Kairouz KC, Heath RJ. Fracture of ply drop-offs in composite structures. Technical report. British Aerospace Airbus; 1997.
[14] Mukherjee A, Varughese B. Development of a specialised finite element for the analysis of composite structures with ply drop-off. Compos Struct 1999;46(1):1–16.
[15] Salpekar SA, Raju IS, O'Brien TK. Strain-energy-release rate analysis of delamination in a tapered laminate subjected to a tension load. J Compos Mater 1991;25:118–41.
[16] Wisnom MR, Dixon R, Hill G. Delamination of asymmetrically tapered composites loaded in tension. Compos Struct 1996;35:309–22.
[17] Wisnom MR, Jones MI, Cui W. Failure of tapered composites under static and fatigue tension loading. Am Inst Aeronaut Astronaut J 1995;33(5).
[18] Yurgartis SW. Measurement of small angle misalignments in continuous fibre composites. Compos Sci Technol 1987;30:279–93.